J. Opt. A: Pure Appl. Opt. **10** (2008) 115003 (6pp) doi:10.1088/1464-4258/10/11/115003

Interferometric testing and description of polarization ray tracing in multi-layer thin films

A M Sadik[1,3], M A El-Morsy[2] and M A Shams-Eldin[2]

[1] Physics Department, Faculty of Science, University of Mansoura, 35516 Mansoura, Egypt
[2] Physics Department, Faculty of Science, University of Mansoura, New Demietta, Egypt

E-mail: adelsa_12@yahoo.com (A M Sadik)

Received 8 May 2008, accepted for publication 4 September 2008
Published 25 September 2008
Online at stacks.iop.org/JOptA/10/115003

Abstract
The production of thin films and their use in different industries necessitates the determination of their optical properties. This paper proposes an extended mathematical model of the output fringe field interference pattern. A general interference formula based on variable-incidence-angle polarizing interference microscopy has been derived for measurement of the optical properties of multi-layer thin film.

In comparison with other well-known interferometric methods, the measurement accuracy of this new method is discussed.

An example of applications to polypropylene sulfide (treated; coated on both sides with PVDC co-polymer) thin film is given.

Keywords: multi-layer thin film, interferometric formula, polarizing interference microscope, variable incidence angle, fringe deflection, directional refractive indices, and thickness

Dedicated to the memory of Professor M A Mabrouk

1. Introduction

Optical characterization of dielectric thin films, particularly the sensitive determination of geometrical thickness and refractive index, is of primary importance for industrial applications. Microinterferometry has been widely employed for non-destructive testing in many fields of applied optics and optical engineering [1, 2]. The most popular microinterferometric methods are based on two-beam interference, like fringe field interferometry.

Fringe field interferometry is a very useful technique for investigation of the optical parameters of fibres, thin films, stripes and such-like objects. These parameters contribute in estimating the optical and structure properties of materials. Various authors used the measured refractive index or birefringence to study some structural parameters [1–5].

The films' thickness and refractive index have been estimated by many authors using IR spectrophotometers and interferometric techniques [6–14]. In most fringe field techniques, both birefringence and directional refractive indices can be calculated from simple formulae on condition that the investigated material thickness is known [1, 2]. Unfortunately accurate measurement of the thickness is not trivial. Also, the methods of double immersion and dual-wavelength are somewhat inconvenient under these conditions [15]. Sadik *et al* [15] and Sadik [16] overcame the problem of the thickness determination uncertainty. They applied the computer-aided variable-incidence-angle Pluta interference (VIAPI) technique. The optical path difference produced by the fibres under investigation, at different incidence angles, is the only quantity that can be measured directly. The directional refractive indices and the thickness of homogeneous and multi-media fibres are then derived from mathematical formulae.

In the present paper, the interference pattern of multi-media thin films has been described by a general interference formula. This formula with the computer-aided variable-incidence-angle Pluta interference (VIAPI) microscope is used for the simultaneous determination of layer thickness and directional refractive indices of multi-media thin films.

[3] Author to whom any correspondence should be addressed.

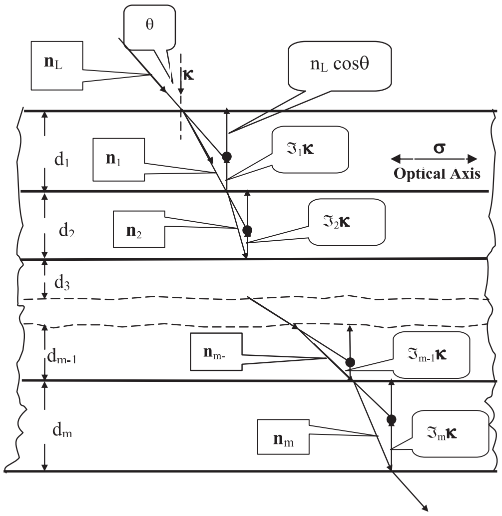

Figure 1. Diagram of the vectors that describes the refraction of rays of light in a multi-media thin film.

2. Theory

2.1. Measurement of the optical properties of each layer of multi-media thin film related to its surrounding medium

We assume a multi-media thin film of m layers as shown in figure 1. It is illuminated by a linearly polarized light and placed diagonally between two crossed polarizers. The directional refractive indices (n_e and n_o) and the thickness (d) of each layer can be calculated as a function of the known refractive index (n_L) of the surrounding medium. The general form of Snell's law for the mth layer can be given as follows:

$$\boldsymbol{n}_m = \boldsymbol{n}_L + \left(\sum_i^m \Im_i\right)\boldsymbol{k}, \tag{1}$$

where $\boldsymbol{n}_m$ ($m = 1, 2, 3, 4, \ldots\ldots$) and $\boldsymbol{n}_L$ represent the incidence and transmitted wavevectors in the mth layer of a multi-media thin film, $\boldsymbol{k}$ is the unit vector normal to the object axis and $\Im_m$ is the scaling constant in the mth layer.

Equation (1) can be rewritten as follows:

$$|\boldsymbol{n}_m|^2 = |\boldsymbol{n}_L|^2 + 2(\boldsymbol{n}_L\cdot\boldsymbol{k})\sum_{i=1}^m \Im_i + \left(\sum_{i=1}^m \Im_i\right)^2. \tag{2}$$

The equation of the index ellipsoid for an extraordinary wave in an anisotropic multi-layer object (m layers) can be expressed as [15]

$$|\boldsymbol{n}_m|^2 = n_{me}^2 - N_m(\boldsymbol{n}_m\cdot\boldsymbol{\sigma})^2, \tag{3}$$

where $\boldsymbol{\sigma}$ is the unit vector parallel to the object axis, $N_m = \frac{n_{me}^2 - n_{mo}^2}{n_{mo}^2}$, where n_{me} and n_{mo} are the extraordinary and ordinary refractive indices of the mth layer, respectively.

Substituting equation (3) into equation (2) we get

$$\left(\sum_{i=1}^m \Im_i\right)^2 + 2(\boldsymbol{n}_L\cdot\boldsymbol{k})\sum_{i=1}^m \Im_i + |\boldsymbol{n}_L|^2 - |\boldsymbol{n}_{me}|^2 + N_m(\boldsymbol{n}_L\cdot\boldsymbol{\sigma})^2 = 0.0, \tag{4}$$

where $\boldsymbol{k}\cdot\boldsymbol{\sigma} = 0.0$ and $\boldsymbol{n}_m\cdot\boldsymbol{\sigma} = (\boldsymbol{n}_L + (\sum_{i=1}^m \Im_i)\boldsymbol{k})\cdot\boldsymbol{\sigma} = \boldsymbol{n}_L\cdot\boldsymbol{\sigma}$.

Solving equation (4), the scaling factor for transmitted light is given by

$$\left(\sum_{i=1}^m \Im_i\right)_\theta = (n_L^2\cos^2\theta + n_{me}^2 - n_L^2 - N_m n_L^2\sin^2\theta)^{1/2} - n_L\cos\theta, \tag{5}$$

where $(\sum_{i=1}^m \Im_i)_\theta = (\sum_{i=1}^m \frac{(\delta_{(i,i-1)\mathrm{e}})_\theta}{d_i})$ and $\delta_{(i,i-1)\mathrm{e}} = \frac{C_{i\mathrm{e}} - C_{(i-1)\mathrm{e}}}{h}\lambda$, where h is the interfringe spacing, $C_{i\mathrm{e}}$ is the extraordinary fringe deflection in the ith layer image, λ is the wavelength of monochromatic light used and d_i is the thickness of the ith layer. Thus

$$\left(\sum_{i=1}^m \frac{(\delta_{(i,i-1)\mathrm{e}})_\theta}{d_i}\right) = [(n_L^2\cos^2\theta + n_{me}^2 - n_L^2 - N_m n_L^2\sin^2\theta)^{1/2} - n_L\cos\theta]. \tag{6}$$

The fringe deflection (C_e) is determined at three different incident angles ($\theta_0 = 0.0°$, θ_1 and θ_2) and substituted into equation (6). The solution of these equations is given by

$$\begin{aligned} n_{me} = n_L &+ \sum_{i=1}^{m-1}\frac{\delta_{\substack{(i,i-1)\mathrm{e}\\ \theta_0}}}{d_i} + \Bigg(\frac{2\delta_{\substack{(m,m-1)\mathrm{e}\\ \theta_0}}}{-C+\sqrt{C^2+S\cdot B}}\Bigg) \\ &\times\left(\sum_{i=1}^{m-1}\frac{\delta_{\substack{(i,i-1)\mathrm{e}\\ \theta_0}}}{d_i}(\sin^2\theta_1 - \sin^2\theta_2)\right. \\ &\times\left(2n_L + \left(\sum_{i=1}^{m-1}\frac{\delta_{\substack{(i,i-1)\mathrm{e}\\ \theta_0}}}{d_i}\right)\right) \\ &+\sum_{i=1}^{m-1}\frac{\delta_{\substack{(i,i-1)\mathrm{e}\\ \theta_1}}}{d_i}\left(2n_L\cos\theta_1 + \left(\sum_{i=1}^{m-1}\frac{\delta_{\substack{(i,i-1)\mathrm{e}\\ \theta_1}}}{d_i}\right)\right)\sin^2\theta_2 \\ &\left.-\sum_{i=1}^{m-1}\frac{\delta_{\substack{(i,i-1)\mathrm{e}\\ \theta_2}}}{d_i}\left(2n_L\cos\theta_2 + \left(\sum_{i=1}^{m-1}\frac{\delta_{\substack{(i,i-1)\mathrm{e}\\ \theta_{21}}}}{d_i}\right)\right)\sin^2\theta_1\right), \end{aligned} \tag{7a}$$

and

$$d_m = \frac{g}{2B}, \tag{7b}$$

where

$$\begin{aligned} S = \big[&(\delta^2_{\substack{(m,m-1)\mathrm{e}\\ \theta_2}} - \delta^2_{\substack{(m,m-1)\mathrm{e}\\ \theta_0}})\sin^2\theta_1 \\ &- (\delta^2_{\substack{(m,m-1)\mathrm{e}\\ \theta_1}} - \delta^2_{\substack{(m,m-1)\mathrm{e}\\ \theta_0}})\sin^2\theta_2\big], \end{aligned}$$

$$\begin{aligned} C = \sin^2\theta_1 &\Bigg(2n_L\delta_{\substack{(m,m-1)\mathrm{e}\\ \theta_0}} + 2\delta_{\substack{(m,m-1)\mathrm{e}\\ \theta_0}}\sum_{i=1}^{m-1}\frac{\delta_{\substack{(i,i-1)\mathrm{e}\\ \theta_0}}}{d_i} \\ &- 2n_L\delta_{\substack{(m,m-1)\mathrm{e}\\ \theta_2}}\cos\theta_2 - 2\delta_{\substack{(m,m-1)\mathrm{e}\\ \theta_2}}\sum_{i=1}^{m-1}\frac{\delta_{\substack{(i,i-1)\mathrm{e}\\ \theta_2}}}{d_i}\Bigg) \\ &+\sin^2\theta_2\Bigg(-2n_L\delta_{\substack{(m,m-1)\mathrm{e}\\ \theta_0}} - 2\delta_{\substack{(m,m-1)\mathrm{e}\\ \theta_0}}\sum_{i=1}^{m-1}\frac{\delta_{\substack{(i,i-1)\mathrm{e}\\ \theta_0}}}{d_i} \\ &+ 2n_L\delta_{\substack{(m,m-1)\mathrm{e}\\ \theta_1}}\cos\theta_1 + 2\delta_{\substack{(m,m-1)\mathrm{e}\\ \theta_1}}\sum_{i=1}^{m-1}\frac{\delta_{\substack{(i,i-1)\mathrm{e}\\ \theta_1}}}{d_i}\Bigg), \end{aligned}$$

$$\begin{aligned}B={}&\left(2n_L\sum_{i=1}^{m-1}\frac{\delta_{\underset{\theta_0}{(i,i-1)\mathrm{e}}}}{d_i}+\left(\sum_{i=1}^{m-1}\frac{\delta_{\underset{\theta_0}{(i,i-1)\mathrm{e}}}}{d_i}\right)^2\right)\\&\times(\sin^2\theta_1-\sin^2\theta_2)\\&+2n_L\cos\theta_1\sin^2\theta_2\sum_{i=1}^{m-1}\frac{\delta_{\underset{\theta_1}{(i,i-1)\mathrm{e}}}}{d_i}+\sin^2\theta_2\left(\sum_{i=1}^{m-1}\frac{\delta_{\underset{\theta_1}{(i,i-1)\mathrm{e}}}}{d_i}\right)^2\\&-2n_L\cos\theta_2\sin^2\theta_1\sum_{i=1}^{m-1}\frac{\delta_{\underset{\theta_2}{(i,i-1)\mathrm{e}}}}{d_i}-\sin^2\theta_1\left(\sum_{i=1}^{m-1}\frac{\delta_{\underset{\theta_2}{(i,i-1)\mathrm{e}}}}{d_i}\right)^2,\end{aligned}$$

and

$$g=(-C+\sqrt{C^2+4S\cdot B}).$$

Also

$$\begin{aligned}N_m={}&\frac{1}{n_L^2}\left(\csc^2\theta_2\left(2n_L\sum_{i=1}^{m-1}\frac{\delta_{\underset{\theta_0}{(i,i-1)\mathrm{e}}}}{d_i}+\left(\sum_{i=1}^{m-1}\frac{\delta_{\underset{\theta_0}{(i,i-1)\mathrm{e}}}}{d_i}\right)^2\right.\right.\\&-2n_L\cos\theta_2\sum_{i=1}^{m-1}\frac{\delta_{\underset{\theta_2}{(i,i-1)\mathrm{e}}}}{d_i}-\left(\sum_{i=1}^{m-1}\frac{\delta_{\underset{\theta_2}{(i,i-1)\mathrm{e}}}}{d_i}\right)^2\\&+\left(\frac{4\delta^2_{\underset{\theta_0}{(m,m-1)\mathrm{e}}}B^2}{g^2}-\frac{4\delta^2_{\underset{\theta_2}{(m,m-1)\mathrm{e}}}B^2}{g^2}\right.\\&+\frac{4\delta_{\underset{\theta_0}{(m,m-1)\mathrm{e}}}n_LB}{g}-\frac{4\delta_{\underset{\theta_2}{(m,m-1)\mathrm{e}}}n_LB\cos\theta_2}{g}\\&+\frac{4\delta_{\underset{\theta_0}{(m,m-1)\mathrm{e}}}B}{g}\sum_{i=1}^{m1}\frac{\delta_{\underset{\theta_0}{(i,i-1)\mathrm{e}}}}{d_i}\\&\left.\left.\left.-\frac{4\delta_{\underset{\theta_2}{(m,m-1)\mathrm{e}}}B}{g}\sum_{i=1}^{m-1}\frac{\delta_{\underset{\theta_2}{(i,i-1)\mathrm{e}}}}{d_i}\right)\right)\right).\end{aligned}\tag{8}$$

The refractive index (n_m) and the thickness (d_m) of the isotropic multi-media thin film ($C_{i\mathrm{e}}=C_{i\mathrm{o}}$) can be determined from the following equations:

$$\begin{aligned}n_m={}&\left\{-n_L^2(\delta_{\underset{\theta_0}{(m,m-1)}}-\delta_{\underset{\theta_1}{(m,m-1)}}\cos\theta_1)\right.\\&-n_L\left(\sum_{i=1}^{m-1}\frac{\delta_{\underset{\theta_1}{(i,i-1)}}}{d_i}(2\delta_{\underset{\theta_0}{(m,m-1)}}\cos\theta_1-\delta_{\underset{\theta_1}{(m,m-1)}})\right.\\&\left.-\sum_{i=1}^{m-1}\frac{\delta_{\underset{\theta_0}{(i,i-1)}}}{d_i}\delta_{\underset{\theta_1}{(m,m-1)}}\cos\theta_1\right)\\&+\delta_{\underset{\theta_0}{(m-1)}}E+\left(-\left(\sum_{i=1}^{m-1}\frac{\delta_{\underset{\theta_1}{(i,i-1)}}}{d_i}\right)^2\delta_{\underset{\theta_0}{(m,m-1)}}\right.\\&\left.\left.+\sum_{i=1}^{m-1}\frac{\delta_{\underset{\theta_0}{(i,i-1)}}}{d_i}\delta_{\underset{\theta_1}{(m,m-1)}}+n_LE\right)\right\}\\&\left\{\left(n_L^2(\delta_{\underset{\theta_0}{(m,m-1)}}-\delta_{\underset{\theta_1}{(m,m-1)}}\cos\theta_1)\right.\right.\\&+\left(\sum_{i=1}^{m-1}\frac{\delta_{\underset{\theta_0}{(i,i-1)}}}{d_i}\delta_{\underset{\theta_0}{(m,m-1)}}-\sum_{i=1}^{m-1}\frac{\delta_{\underset{\theta_1}{(i,i-1)}}}{d_i}\delta_{\underset{\theta_1}{(m,m-1)}}\right)\\&\left.\left.-E\right)\right\}^{-1}\end{aligned}\tag{9a}$$

and

$$\begin{aligned}d_m={}&\left\{\left(-n_L(\delta_{\underset{\theta_0}{(m,m-1)}}-\delta_{\underset{\theta_1}{(m,m-1)}}\cos\theta_1)\right.\right.\\&-\left(-\sum_{i=1}^{m-1}\frac{\delta_{\underset{\theta_0}{(i,i-1)}}}{d_i}\delta_{\underset{\theta_0}{(m,m-1)}}+\sum_{i=1}^{m-1}\frac{\delta_{\underset{\theta_1}{(i,i-1)}}}{d_i}\delta_{\underset{\theta_1}{(m,m-1)}}\right)\\&\left.\left.+E\right)\right\}\left\{\left(\sum_{i=1}^{m-1}\frac{\delta_{\underset{\theta_0}{(i,i-1)}}}{d_i}\right)^2-\left(\sum_{i=1}^{m-1}\frac{\delta_{\underset{\theta_1}{(i,i-1)}}}{d_i}\right)^2\right.\\&\left.+2n_L\left(\sum_{i=1}^{m-1}\frac{\delta_{\underset{\theta_0}{(i,i-1)}}}{d_i}-\sum_{i=1}^{m-1}\frac{\delta_{\underset{\theta_1}{(i,i-1)}}}{d_i}\cos\theta_1\right)\right\}^{-1},\end{aligned}\tag{9b}$$

where

$$\begin{aligned}E={}&\left(n_L(\delta_{\underset{\theta_0}{(m,m-1)}}\cos\theta_1-\delta_{\underset{\theta_1}{(m,m-1)}})\right.\\&\left.+\left(\sum_{i=1}^{m-1}\frac{\delta_{\underset{\theta_1}{(i,i-1)}}}{d_i}\delta_{\underset{\theta_0}{(m,m-1)}}-\sum_{i=1}^{m-1}\frac{\delta_{\underset{\theta_0}{(i,i-1)}}}{d_i}\delta_{\underset{\theta_1}{(m,m-1)}}\right)\right).\end{aligned}$$

The thickness and the refractive index of each layer of the birefringent and isotropic multi-media thin film can be determined using equations (7), (8) and (9). The accuracy of these measurements depends on the measuring accuracy of the extraordinary fringe deflections ($C_{i\mathrm{e}}$) in each layer at different angles of incidence (θ).

3. Experimental details

3.1. Measuring technique

The polarizing interference (PI) microscope developed by Pluta [2] is much more complicated. This microscope is used to carry out observations of various micro-objects that produce either a phase shift or an amplitude of the transmitted light. The microscope is applied for measuring the optical path difference (phase shift), gradient of the optical path difference, thickness, refractive index, birefringence and other physical quantities of the fibres, stripes and thin films.

The basic optical elements of this system are shown in figure 2. Rotating the birefringent Wollaston prism W_o about the optical axis of the objective (Obw) changes the degree of shearing and direction of image duplication, while the direction of interference fringes in the image plane and the interfringe spacing remain unchanged. Such independence of the interfringe spacing on image duplication is an advantage

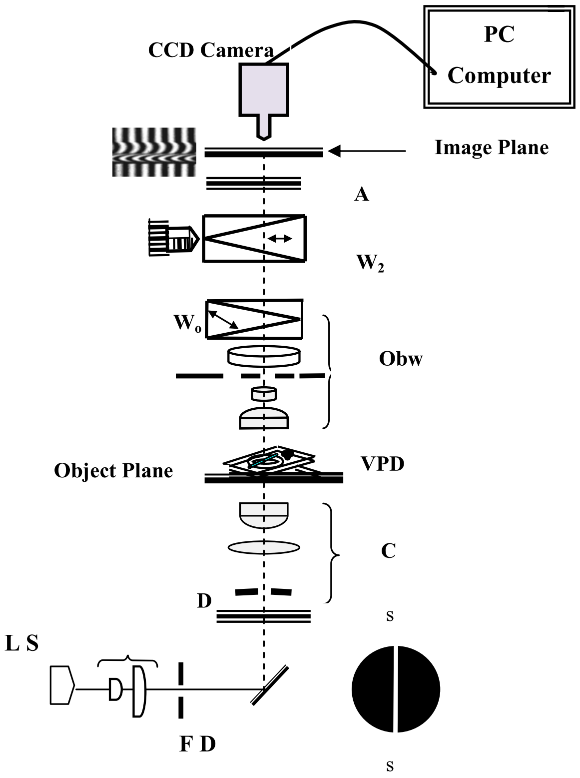

Figure 2. Schematic diagrams of the experimental set-up of the Pluta birefracting microinterferometer: LS—light source, Col—collimator, FD—field diaphragm, P—polarizer, D—regular slit diaphragm, Π—object plane, VPD—variable prismatic device, W_o—rotatable Wollaston prism, W_2—tube Wollaston prism, A—analyzer, Π\—image plane, CCD camera.

of this interferometric system. Assume that the objective birefringent prism (W_o) is adjusted to the leftmost or right-crossed position with respect to the tube birefringent prism (W_2). The multi-layer thin film that is placed in the object plane and surrounded by a liquid is oriented at right angles to the interference fringes of the interference empty field. The variable prismatic device (VPD) is used to change the angle of incidence of the monochromatic light with respect to the investigated object axis. The output field of the microscope is scanned by a CCD camera and the interference image is automatically analysed and processed.

3.2. Materials

In the present work, the investigated sample is a polypropylene (treated; coated on both sides with polyvinylidene chloride (PVDC) co-polymer) thin film. The polyvinylidene chloride is applied as a water-based coating to other plastic films such as polypropylene and polyester. This coating increases the barrier properties of the film, reducing the permeability of the film to oxygen, water vapour and flavours, and thus extending the shelf life of the objects inside the package. Also, this coating increases the physical protection of the objects enclosed in the package from shock, vibration, compression, temperature, etc. The total film thickness is measured at ten positions using a digital micrometre and found to be 22.5 μm with an accuracy of approximately 5%. The values of the melting point and T_g of this thin film are 170 and 225–250 °C, respectively.

3.3. Results and discussion

In transverse interferometric methods, the investigated object is illuminated transversally to its axis. The set-up of the optical apparatus for producing fringe field interference (FFI) patterns of a polypropylene (treated; coated on both sides with PVDC co-polymer) thin film is shown in figure 2. The polarizer P and analyzer A are crossed and their directions of light vibrations form an angle of 45° with the axis of the thin film. The slit S is oriented to the thin film axis by an angle 90°. The FFI patterns of the output field of the microscope are captured by a CCD camera for further automatic processing and analysis by the computer system. The thin film axis should be oriented at right angles to the interference fringes of the interference empty field.

Figure 3(a) displays wavefront shear fringe field interference and total duplicated images of the polypropylene (treated; coated on both sides with PVDC co-polymer) thin film captured by the CCD camera at incidence angle $\theta = 5°$. This thin film is immersed in a liquid of refractive index $n_L = 1.58737 \pm 2 \times 10^{-5}$ at temperature 28 °C and illuminated by a monochromatic light of wavelength $\lambda = 546 \pm 0.1$ nm. The microscope objective of magnifying power/numerical aperture 10 × /0.24 is used. It should be noted that the total duplicated images of the thin film must be mutually sheared in at least 50%. Therefore, the width of the investigated thin film is restricted and for the microscope Ob 10 × /0.24 may not be greater than 64 μm [2]. The width of the present investigated thin film is greater than 100 μm. Therefore, the shearing of the total duplicated images of this thin film are overlapped in a certain area (overlapping area) as shown in the schematic diagram, figure 3(b).

When the birefracting microinterferometer is adapted to the subtractive configuration of prisms, a non-duplicated interferogram may be obtained. Figure 3(d) shows a microinterferogram of the differentially sheared (non-duplicated) images of the film to determine the mean birefringence directly. It is very clear that the interference fringes are straight through the immersion liquid and the film, which confirms that the birefringence is equal to zero.

From these microinterferograms, it seems that this investigated thin film is an isotropic object with skin–core structure ($C_{ei} = C_{oi} = C_i$, where C_{ei} and C_{oi} are the extraordinary and ordinary fringe deflections, respectively). So, the refractive index (n_m) and the thickness (d_m) of this isotropic thin film can be determined by using equations [9].

A set of measurements of fringe deflections (C_i) in the fibre images for light vibrating parallel to the fibre axis at different incidence angles ($\theta_i \pm 1$ s) is performed. The fringe deflection (C_i) in each layer and the interfringe spacing (h) are measured in pixels using the image processing technique. Also, it is important to note that the interfringe spacing of the liquid fringes is not affected by the magnifying power of the microscope objective. The optical path differences for

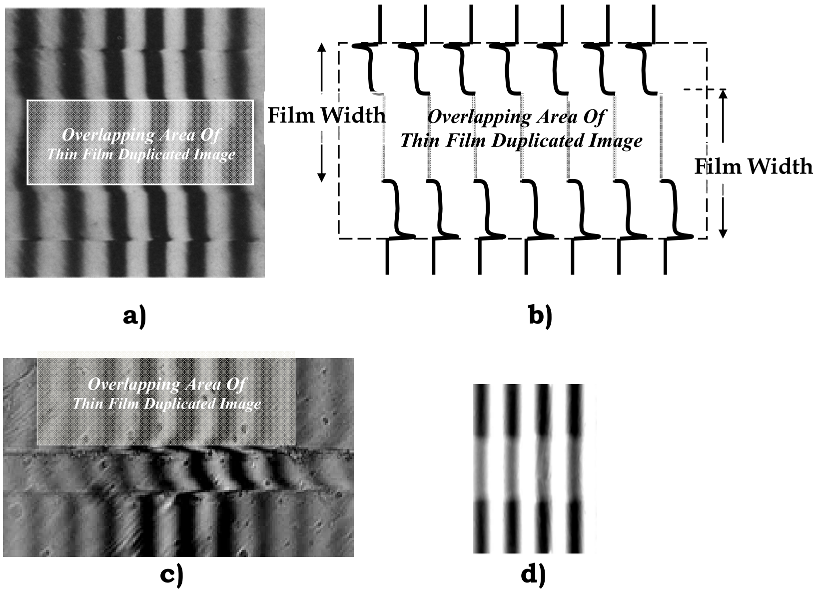

Figure 3. Fringe field interference with variable wavefront shear and images of a polypropylene (treated; coated on both sides with PVDC co-polymer) thin film for an incidence angle of 5° with the film surface; the objective prism W_o is adjusted at the crossed ((a) and (c)) and subtractive (d) position in relation to the tube birefringent prism W_2. The refractive index of the immersion liquid in ((a) and (d)) is 1.587 37 and in (c) is 1.557 50. Objective PI 10 × /0.24. (b) is the schematic diagram of the wavefront shear fringe field interference and total duplicated images of a polypropylene thin film.

Table 1. The average values of refractive index and thickness of each layer of a polypropylene (treated; coated on both sides with PVDC co-polymer) thin film using the new presented interference and both conventional standard and double-immersion interference methods.

	Skin layer		Inner layer	
	$2d_1$ (μm)	n_s	d_2 (μm)	n_c
New interference formula (equations (9))	6.61	1.598 69	15.39	1.586 86
	$\Delta d(n_L, \theta, \delta) = \pm 24 \times 10^{-2}$ and $\Delta n(n_L, \theta, \delta) = \pm 13 \times 10^{-5}$			
Standard interference formula (see [16])	6.82	1.5987	15.54	1.5869
	$\Delta d(n_L) = \pm 51 \times 10^{-2}$ and $\Delta n(n_L, d, \delta) = \pm 4.3 \times 10^{-4}$			
Double-immersion interference formula (equations (10))	6.33	1.5986	15.48	1.5867
	$\Delta d(n_L, \delta) = \pm 56 \times 10^{-2}$ and $\Delta n(n_L, \delta) = \pm 4.8 \times 10^{-4}$			

each layer ($\delta_i = \pm 25 \times 10^{-4}\ \lambda$) are determined at these angles. Having determined these optical path differences at two different incidence angles, the refractive index and thickness of skin and inner layers are calculated when the presented interference formula is applied (substituted into equations (9)). This procedure is repeated for another two different incidence angles. The average values of the refractive index and thickness of each layer of the polypropylene thin film are determined and the results are shown in table 1. The global errors in determination of the refractive indices $\Delta n(n_L, \theta, \delta)$ and the layer thickness $\Delta d(n_{L,}\theta, \delta)$ are estimated and found to be $\pm 13 \times 10^{-5}$ and $\pm 24 \times 10^{-2}$, respectively.

The measurements of these optical parameters determined with the presented interference formula are compared with the well-known standard and double-immersion interference formulae [2]. These well-known interference formulae are used to determine the refractive index and the thickness of each layer of a polypropylene (treated; coated on both sides with PVDC co-polymer) thin film. The procedures of the standard interferometric method and the well-known conventional interference formula are given elsewhere [16]. The procedures of the second interferometric method depend on immersing the thin film in two media whose refractive indices, n_{L_1} and n_{L_2}, are exactly known. Thus, the refractive index and the thickness of each layer of a thin film can be simultaneously determined using the following derived equations:

$$n_m = \frac{n_{L_1} \underset{\theta=0.0}{\delta_{m_2}} - n_{L_2} \underset{\theta=0.0}{\delta_{m_1}} + 2d_{m-1}(n_{L_2} - n_{L_1})n_{m-1}}{\underset{\theta=0.0}{\delta_{m_2}} - \underset{\theta=0.0}{\delta_{m_1}} + 2d_{m-1}(n_{L_2} - n_{L_1})},$$

$$\text{and} \qquad d_m = \frac{\underset{\theta=0.0}{\delta_{m_2}} - \underset{\theta=0.0}{\delta_{m_1}} + 2d_{m-1}(n_{L_1} - n_{L_2})}{(n_{L_1} - n_{L_2})} \tag{10}$$

$$m \begin{cases} 1 & \text{for skin layer } (d_0 = 0.0) \\ 2 & \text{for inner layer} \end{cases}$$

where $\delta_{m_1}(= \frac{C_{m_1}}{h}\lambda)$ and $\delta_{m_2}(= \frac{C_{m_2}}{h}\lambda)$ are the optical path differences produced by the mth layer of a thin film immersed in the first liquid of refractive index n_{L_1} and then in the second one of refractive index n_{L_2}, respectively. It is important to note that both immersion liquids must be inactive media and the first of them must be removed completely or the investigated sample is replaced by another one of the same thin film before applying the second immersed medium.

Figure 3(c) displays the wavefront shear fringe interferogram of another sample of the same investigated thin film but immersed in a liquid of refractive index $1.557\,50 \pm 2 \times 10^{-5}$. The optical path differences in each layer of the thin film for a given refractive index of the liquid are determined. Having determined these optical path differences, the refractive index and the thickness of the skin and the inner layers of the investigated thin film can be determined when the well-known standard and double-immersion interference formulae are applied and the results are shown in table 1. From the results shown in table 1, it is worth noting that the new presented interference formulae (equations (8) and (9)) and both of the conventional standard and double-immersion interference formulae give approximately the same results. Using the new presented interference and conventional double-immersion methods, it is not necessary to calibrate the optical system and translate the pixels to the real values in microns. Also, they enable both the refractive index and the thickness of each layer of film to be simultaneously determined, but on using the conventional standard method [16] the optical system needs to be calibrated. This means that it is necessary to translate the pixels to real values in microns to measure the real thickness of each layer of thin film, applying the image processing system (intensity distribution measurement method). Therefore the global errors in the determination of the refractive indices $\Delta n(n_L, d, \delta)$ and thickness ($\Delta d(n_L)$) were found to be less than $\pm 10^{-4}$ and $\pm 40 \times 10^{-2}$, respectively [16].

Using both conventional standard and presented interference techniques, the same part of the length of the same thin film is investigated. So, the uncertainty in measurements of the thin film optical parameters can be minimized, but on using the conventional double-immersion technique we need to remove completely the first immersed medium before applying the second medium or replace the investigated sample by another one of the same thin film. Sometimes the fringe deflections inside the images of each layer of the thin film are changed when the thin film under investigation is translated along its axis. This means that the films' thickness is not stable along its axis (manufacturing defect). This is the disadvantage of the double-immersion technique. Also, the procedures of this technique are time-consuming compared to the newly presented and standard techniques.

The disadvantages of the conventional standard technique are discussed elsewhere [15, 16]. Finally, the newly presented interference formula gives very similar results to the conventional standard and double-immersion interference formulae but the accuracy of the former is significantly higher, as shown in table 1.

4. Conclusions

The present derived interference formula gives a possibility to measure simultaneously the refractive index and the thickness of each layer of a multi-media thin film with an accuracy of $\pm 13 \times 10^{-5}$ and $\pm 24 \times 10^{-2}$, respectively. This accuracy is not inferior to the well-known conventional interferometric methods of index and thickness measurements. Also, measurement procedures are automated and do not require much time. Moreover, using the present derived interference formula the optical system does not need to calibrate and translate the pixels to real values in microns. This means that the present interference formula overcomes the problem of the thickness determination uncertainty. Also, this interference formula can be applied to refractive index and thickness measurement for each layer of the birefringent multi-media thin film.

References

[1] Barakat N and Hamza A A 1990 *Interferometry of Fibrous Materials* (Bristol: Hilger)
[2] Pluta M 1993 *Advanced Light Microscopy* (Amsterdam: Elsevier)
[3] Hong S U, Chang C and Stein R S 1975 *J. Polym. Sci.* B **13** 1447
[4] Rietsch F, Duckett R A and Ward I M 1979 *Polymer* **20** 1133
[5] Stéphanie P, Bernard J and Gérard F 1999 *J. Opt. Eng.* **36** 983
[6] Matsuo H, Hno K and Kondo M 1963 *J. Appl. Polym. Sci.* **7** 1833
[7] Harrick N J 1971 *Appl. Opt.* **10** 2344
[8] Goodman A M 1978 *Appl. Opt.* **17** 2779
[9] Aleksandrov S A and Chernyh I V 1992 *Proc. SPIE* **1756** 221
[10] Pluta M 1992 *Proc. SPIE* **1846** 72
[11] Hernandez M, Juarez A and Hernandez R 1999 *Superficies Vacio* **9** 283
[12] Hamza A A, Mabrouk M A, Ramadan W A and Emara A M 2003 *Opt. Commun.* **225** 341
[13] Shabana H M 2004 *Polym. Test.* **23** 695
[14] Nasr A M and Sadik A M 2001 *J. Opt. A: Pure Appl. Opt.* **3** 200
[15] Sadik A M, Ramadan W A and Litwin D 2003 *J. Meas. Sci. Technol.* **14** 1753
[16] Sadik A M 2007 *J. Meas. Sci. Technol.* **18** 2712